Experimental Neurology 237 (2012) 199–206

Contents lists available at SciVerse ScienceDirect

Experimental Neurology

journal homepage: www.elsevier.com/locate/yexnr

A novel zebrafish model of hyperthermia-induced seizures reveals a role for TRPV4 channels and NMDA-type glutamate receptors

Robert F. Hunt, Gabriela A. Hortopan, Anna Gillespie, Scott C. Baraban *

Epilepsy Research Laboratory, Department of Neurological Surgery, Biomedical Graduate Program, University of California San Francisco, San Francisco, CA 94143, USA

ARTICLE INFO

Article history:
Received 16 March 2012
Revised 31 May 2012
Accepted 16 June 2012
Available online 24 June 2012

Keywords:
Seizure
Epilepsy
In vivo
Pharmacology
Extracellular recording
Heat
Temperature

ABSTRACT

Febrile seizures are the most common seizure type in children under the age of five, but mechanisms underlying seizure generation in vivo remain unclear. Animal models to address this issue primarily focus on immature rodents heated indirectly using a controlled water bath or air blower. Here we describe an in vivo model of hyperthermia-induced seizures in larval zebrafish aged 3 to 7 days post-fertilization (dpf). Bath controlled changes in temperature are rapid and reversible in this model. Acute electrographic seizures following transient hyperthermia showed age-dependence, strain independence, and absence of mortality. Electrographic seizures recorded in the larval zebrafish forebrain were blocked by adding antagonists to the transient receptor potential vanilloid (TRPV4) channel or N-methyl-d-aspartate (NMDA) glutamate receptor to the bathing medium. Application of GABA, GABA re-uptake inhibitors, or TRPV1 antagonist had no effect on hyperthermic seizures. Expression of vanilloid channel and glutamate receptor mRNA was confirmed by quantitative PCR analysis at each developmental stage in larval zebrafish. Taken together, our findings suggest a role of heat-activation of TRPV4 channels and enhanced NMDA receptor-mediated glutamatergic transmission in hyperthermia-induced seizures.

Introduction

Febrile seizures are triggered by a rise in body temperature (i.e., hyperthermia or fever) in the absence of CNS infection or metabolic disorder (Stafstrom, 2002). They are the most common form of childhood seizures, occurring in up to 6% of children under five years of age (Annegers et al., 1987; Berg et al., 1992; Hauser and Hersdorffer, 1990; Stafstrom, 2002; Verity et al., 1985). Although febrile seizures typically cease during childhood and are often considered benign, seizure recurrence is relatively common (Berg et al., 1997). Febrile seizures can also be associated with increased risk for temporal lobe epilepsy or cognitive disabilities later in life (Annegers et al., 1987; Dubé et al., 2006, 2009b, 2010; Shinnar, 1998). Therefore, a better understanding of potential mechanisms underlying seizure generation during hyperthermia is clinically important and might lead to preventative strategies given at the time of fever.

Several studies have used experimental hyperthermia to raise brain temperature and elicit seizure-like activity in immature rodents. These studies offer valuable insight into long-term molecular and functional consequences of febrile seizures that might contribute to epileptogenesis or increased neuronal excitability. For example, chronic changes in hyperpolarization-activated, cyclic nucleotide-gated (HCN) channels (Brewster et al., 2002; Chen et al., 1999, 2001; Richichi et al., 2008) and GABAergic transmission (Chen et al., 1999; Tsai and Leung, 2006) have been reported after prolonged hyperthermia. Acute increase in temperature has also been shown to produce epileptiform discharges and spreading depression in hippocampal slices and cultured neurons from immature rats (Tancredi et al., 1992; Wu and Fisher, 2000). However, it remains unclear how an elevation in temperature promotes seizure generation in the developing brain in vivo. This question is difficult to resolve using current rodent models of febrile seizures due to the technical limitations of examining acute changes in excitability during febrile seizure generation in immature rats in vivo (Baram, 2002).

Members of the transient receptor potential vanilloid (TRPV) subfamily of non-specific cation channels are temperature-gated ion channels (Kauer and Gibson, 2009; Patapoutian et al., 2003) with high Ca^{2+} permeability that might promote synchronous network activity in response to a rise in brain temperature. TRPV1 and 4 are expressed in the mammalian brain (Bhaskaran and Smith, 2010; Caterina et al., 1997; Shibasaki et al., 2007; Zsombok et al., 2012) and in zebrafish (Mangos et al., 2007; Saito and Shingai, 2006) where they have been shown to regulate neuronal excitability at physiological temperatures. Heat-activation of TRPV4 has been shown to depolarize and evoke inward, excitatory currents in hippocampal neurons (Shibasaki et al., 2007) and cortical astrocytes (Benfenati et al., 2007). Similarly, pharmacological activation of TRPV1 triggers glutamate release in vitro (Doyle et al., 2002; Jin et al., 2004; Peters et al., 2010), a response that can be blocked by lowering basal temperature (Peters et al., 2010). Enhanced

* Corresponding author at: Box 0112, Dept. of Neurological Surgery, 513 Parnassus Avenue, San Francisco, CA 94143, USA.
E-mail address: scott.baraban@ucsf.edu (S.C. Baraban).

0014-4886/$ – see front matter © 2012 Elsevier Inc. All rights reserved.
doi:10.1016/j.expneurol.2012.06.013

TRPV1 channel activation is also associated with increases in excitatory synaptic input to dentate gyrus granule cells in an acquired epilepsy model (Bhaskaran and Smith, 2010). Given these findings, activation of thermosensitive TRPV channels in response to an increase in brain temperature might promote abnormal neuronal excitability and the subsequent exacerbation of excitability via increased glutamate-mediated synaptic transmission resulting in febrile seizures. To address these issues, we developed a novel in vivo model of acute hyperthermia (HT)-induced seizures using larval zebrafish. Using this simple vertebrate model, we completed a series of pharmacological studies to examine potential mechanisms contributing to the generation of acute electrographic seizures following transient temperature elevation. Quantitative PCR studies were used to assess the developmental expression profile for TRPV channels and glutamate receptor subunits.

Methods

Animals and maintenance

Wild-type zebrafish (*Tu*, *WIK*, *TL*) were obtained from the Zebrafish International Resource Center (Eugene, OR; http://zebrafish.org/zirc/fish/lineAll.php). Adult zebrafish were maintained according to standard procedures (Westerfield, 1993), and following the guidelines approved by the University of California, San Francisco Institutional Animal Care and Use Committee. Zebrafish embryos and larvae were maintained in egg water (0.03% Instant Ocean) unless otherwise stated.

Electrophysiology

To obtain stable physiological recordings, zebrafish larvae were briefly anesthetized in tricaine, paralyzed in α-bungarotoxin and immobilized in 1.2% low-melting temperature agarose in zebrafish egg water. Larvae were embedded so that the dorsal aspect of the brain was accessible for electrode placement. Embedded larvae were bathed in egg water and visualized using an Olympus BX50 microscope (Olympus America Inc., Center Valley, PA). Under direct visual guidance, a glass microelectrode (<1.2 mm tip diameter, 2–7 MΩ) was placed in the forebrain along the midline where most neuronal somas are located. Electrodes were filled with 2 M NaCl and electrical activity was recorded using a Patch Clamp PC-505B amplifier (Warner Instruments, Hamden, CT). Voltage records were low-pass filtered at 2 kHz (−3 dB, 8-pole Bessel), Notch filtered at 60 Hz, digitized at 10 kHz using a Digidata 1300 A/D interface, and stored on a PC computer running Axoscope software (Molecular Devices, Sunnyvale, CA). Electrophysiological recordings were coded and analyzed post hoc using Clampfit software (Molecular Devices). Drugs were added directly to the bathing medium at a perfusion rate of ~5 ml/min. An in-line solution heater (Model SH-27B) and an automatic temperature controller (Model TC-324B, Warner Instruments) were used to control bath temperature; "set temp" was held at 45 C and output voltage at 10 mV. Temperature controller was activated for precisely 3 min. Bath temperature was monitored using a probe placed in the agar used to embed the zebrafish larvae. Statistical comparisons were made using a Student's *t*-test or Mann–Whitney Rank Sum test (when an equal variance test failed); significance was taken as $p \leq 0.05$.

RNA isolation, PCR, cloning, and sequencing

Total RNA was isolated from pools of larvae (10 fish/pool) at different stages of development (2–7 dpf) using RNeasy®Mini Kit (Qiagen), treated by RNase-free DNase to remove possible genomic DNA contamination and quantified with Nanodrop ND-1000 Spectrophotometer. 1 μg RNA was used to generate cDNA using SuperScript™ III First-Strand Synthesis System (Invitrogen) according to the manufacturer's protocol. Primer pairs, forward and reverse, were designed using Primer 3 web software (http://frodo.wi.mit.edu/primer3/) for each investigated gene (primer sequences are available in Table 1). cDNA was amplified in a polymerase chain reaction (PCR), each reaction cycle (32 loops) consisted of incubations at 94 °C (30 s), 60 °C (30 s), and 72 °C (60 s) using Phusion High-Fidelity Master Mix (Thermo Scientific, Finnzymes). A 1.2% agarose gel electrophoresis stained with ethidium bromide was used to separate the PCR products which were further cloned using TOPO TA Cloning System (Invitrogen) according to the manufacturer's specifications. DNA sequencing was performed by Elim Biopharmaceuticals, Inc. (Hayward, CA).

Quantitative real-time PCR (qPCR)

The qPCR reactions were performed using SybrGreen fluorescent master mix on StepOnePlus™ Real-Time PCR System (Applied Biosystems). Primers were designed using Primer Express v3.0 (Applied Biosystems) and synthesized locally (Table 2). A total of 30 samples (sample = pool of 10 zebrafish embryos; 5 samples/stage of development = 5 biological replicates) were run in triplicate in 1× SYBR green master mix, 10 μM of each primer and RNAse free water for a final volume of 25 μl. To determine primer efficiencies, serially diluted pooled cDNAs, also assayed in triplicate, were used to construct standard curves and the efficiency was calculated according to the following formula: $E = 10^{[-1/\text{slope}]}$. For each set of primers, the standard curve was prepared using 4-fold serial dilutions (5 standards in triplicate: 1/1; 1/4; 1/16; 1/64; 1/256). Efficiencies, slope of the curves and the correlation coefficient are shown in Table 3. Primer sets with standard curve slope values ranging from −3.3 to −3.7 were accepted.

Samples without reverse transcriptase and samples without RNAs were run for each reaction as negative controls. Cycling parameters were as follows: 50 °C × 2 min, 95 °C × 10 min, then 35 cycles of the following 95 °C × 15 s, 60 °C × 1 min. At the end of the PCR reactions, samples were subjected to a dissociation curve analysis (dissociation step was performed at 95 °C × 15 s, 60 °C × 20 s, and 95 °C × 15 s) to confirm specificity of amplification. Quantification cycle values [Cq], provided from real-time qPCR instrumentation, were imported into a Microsoft Excel spreadsheet for additional analysis. Raw data were analyzed using qCalculator software (programmed by Ralf Gilsbach, Germany) that estimates qPCR efficiency, and the relative gene expression between samples after normalization with the chosen reference gene (β-actin) basing on both the comparative ddCT (Livak and Schmittgen, 2001) and the efficiency-based (Pfaffi, 2001) methods. Both types of analyses gave similar results. Significant differences were considered at P value ≤ 0.05 (Student's *t* test).

Results

Characteristics of hyperthermic seizures in larval zebrafish

Transient elevation of bath temperature resulted in abnormal electrographic seizure activity in 100% of agar-embedded larval zebrafish (n = 104; Fig. 1). Hyperthermia (HT)-induced seizures were initially associated with "ictal-like" multi-spike, large amplitude, long-duration burst discharges (>1 s; Fig. 1B) that progressed to include shorter, small amplitude, high frequency events (Fig. 1C). Field potentials recorded in the forebrain during acute hyperthermia were similar in waveform to those previously observed in larval zebrafish exposed to pentylenetetrazole, 4-aminopyridine or linopirdine (Baraban et al., 2005, 2007; Chege et al., 2012). HT seizure durations between 2 and 7 min were observed. Seizure duration increased with age to a peak around 5 dpf (Figs. 2A–B). Seizures did not show any strain sensitivity (Fig. 2B, inset). Agar bath temperature at which the first electrographic seizure-like event was observed was 25.5 ± 0.3 °C, from a baseline room temperature level of 22 ± 0.1 °C. Temperature thresholds for initiation of seizure activity did not vary with larval age between 3 and 7 days post-fertilization (Fig. 2C); peak agar temperature reached was similar for all developmental stages 33.5 ± 0.3 °C (Fig. 2D). Seizures

Table 1
Primers used for amplification, cloning and sequencing. Primer's sequences and GeneBank accession number for each investigated genes in conventional RT-PCR.

Gene name	Gene symbol	GeneBank	Sequence
Glutamate receptor, ionotropic, AMPA 1a	gria1a	NM_205598	F, 5′ GTTCGCAGTTCTCCAAAGGA 3′ R, 5′ CGTCAGGTCAATGTCCAAAA 3′
Glutamate receptor, ionotropic, AMPA 2a	gria2a	NM_131894	F, 5′ TGGGGAAGAATGTGAAGAGC 3′ R, 5′ TGTCCTTCGTCCTTTCTCGT 3′ F, 5′ CACGTGTCCTTCATCACACC 3′ R, 5′ TCATCACTTGCACAGCATCA 3′
Glutamate receptor, ionotrophic, AMPA	gria3b	NM_198360	F, 5′ AGGCTCTGGAGGAAAAGGAG 3′ R, 5′ GCAGCCAGATCCACACAGTA 3′ F, 5′ CCTCCTTTGTCACACCCAGT 3′ R, 5′ AATGTCGATGCCTTGACTCC 3′
Glutamate receptor, ionotropic, N-methyl D-aspartate 1a	grin1a	BC124078	F, 5′ GGAGTCAAGGCATCGACATT 3′ R, 5′ CGGCTCACTAGGAAAAGCAC 3′ F, 5′ GTGTGGGCTGGTTTTGCTAT 3′ R, 5′ GCATTGCTTCTGGAGTCACA 3′
Glutamate receptor, ionotropic,, NMDA2B	grin2b	NM_001128337	F, 5′ AGTCACCCATAAGCCAAACG 3′ R, 5′ CTCAAAGAGCTCCTGGATGG 3′ F, 5′ GAGACCGGGATCAGTGTCAT 3′ R, 5′ TCCTCCATCTCACCATCTCC 3′
Transient receptor potential cation channel, subfamily V, member 1	trpv1	EU423314	F, 5′ TCGCCCAGATATTGGACTTC 3′ R, 5′ CAGGCCATAGTCCCACTCAT 3′ F, 5′ GCCTGTGGGAAATTCTTTCA 3′ R, 5′ CGCAAATTGATCCCACTTCT 3′
Transient receptor potential cation channel, subfamily V, member 4	trpv4	NM_001042730	F, 5′ CCAAGACCAAGTTGGAGGAA 3′ R, 5′ AGCTCAAGGCAAGACAGAGC 3′ F, 5′ AAGAGGCTGACCGATGAAGA 3′ R, 5′ CGGGTAGAGTTTGGCACATT 3′ F, 5′ ACTGGGCTTATGGACCAGTG 3′ R, 5′ CACAGACACGTAGGCCTCAA 3′

were repeatable in the same fish and did not lead to death in any trial. Seizures were not observed in recordings made at room temperature (Fig. 2D).

Pharmacology of hyperthermic seizures in larval zebrafish

To examine potential mechanisms, a baseline HT seizure recording was obtained in separate groups of fish between 5 and 7 dpf. Solution was then exchanged for a test compound and allowed to equilibrate into the agar for ~45 min, as described previously (Baraban et al., 2005), followed by a second HT challenge in the same fish; only one drug manipulation was performed per fish. Representative extracellular recordings for these types of experiments are shown in Fig. 3. GABA (1 mM) or the GABA re-uptake inhibitors nipecotic acid (1 mM) and NO-711 (100 μM) did not alter HT-induced seizure duration. RN-1734 (0.5–1 mM), a TRPV4 channel antagonist, produced a significant reduction of HT seizure activity (Fig. 3C); capsazapine (100 μM; Fig. 3D), a TRPV1 channel antagonist had no effect. MK-801 (1 mM; Fig. 3B), a competitive NMDA receptor antagonist, or ifenprodil (1 mM), a NR1 and NR2B specific NMDA receptor antagonist, significantly reduced HT-induced seizure duration. Temperature thresholds for the initiation of seizure activity or peak temperature reached were not altered by any drug manipulation.

Channel and receptor expression in larval zebrafish

Quantitative PCR (qPCR) was used to evaluate the expression levels for glutamate receptor subunits and TRPV channels between 2 and 7 dpf. Zebrafish *gria* (AMPA-type) and *grin* (NMDA-type) receptor subunit expression was very low at 2 days post-fertilization, a developmental stage where larvae are just beginning to emerge from the chorion (Figs. 4A–B). Glutamate receptor subunit expression

Table 2
Primers used for qPCR assay. Real-time qPCR primer sequences and amplicon size for each gene of interest and for the endogenous gene used in SYBR Green assay. F, Forward; R, reverse.

Gene name	Gene symbol	Sequence	Amplicon(bp)
Beta-actin	β-act	F, 5′ CATCCATCGTTCACAGGAAGTG 3′ R, 5′ TGGTCGTTCGTTTGAATCTCAT 3′	83
Glutamate receptor, ionotropic, AMPA 1a	gria1a	F, 5′ AAGTTCCCAAGCGAAGACTGAA 3′ R, 5′ GTTCTGGAAAGCTGTGGACATG 3′	80
Glutamate receptor, ionotropic, AMPA 2a	gria2a	F, 5′ GGAGACTGCCTGGCCAATC 3′ R, 5′ TCCACACGCACCTGTTTAAGAG 3′	80
Glutamate receptor, ionotrophic, AMPA	gria3b	F, 5′ GCAGGTTGTGACACTTGGAAAG 3′ R, 5′ AGGAAGACCTTGTCCAGGCTAA 3′	93
Glutamate receptor, ionotropic, N-methyl D-aspartate 1a	grin1a	F, 5′ CGAGCCCAAGATTGTGAACA 3′ R, 5′ CCTGGGTGACGGCATCTTTA 3′	80
Glutamate receptor, ionotropic,, NMDA2B	grin2b	F, 5′ AGTCGGGTAAATTGGATGCATT 3′ R, 5′ CCAGCTTACAGCCCTCATCAC 3′	81
Transient receptor potential cation channel, subfamily V, member 1	trpv1	F, 5′ TTGGTGAGCTGCCCTTGTC 3′ R, 5′ GCCTGGTGAGGGTTTTCCAT 3′	81
Transient receptor potential cation channel, subfamily V, member 4	trpv4	F, 5′ GCCCAGAGATGAGGGTGGAT 3′ R, 5′ CCATGTCTGGTTGGTTGGTACA 3′	80

Table 3
Slope, efficiency, intercept and correlation coefficient output from qCalculator software. qPCR efficiencies for all genes, slope of the curves, intercept and the correlation coefficient were estimated using the equation E = 10[−1/slope] (qCalculator software) using the CT values obtained by the standard serial dilutions assayed in triplicate (4 fold serial dilution). CT: cycle threshold; β-act: beta-actin; gria1a: glutamate receptor, ionotropic, AMPA 1a; gria2a: glutamate receptor, ionotropic, AMPA 2a; gria3b: glutamate receptor, ionotrophic, AMPA; grin1a: glutamate receptor, ionotropic, N-methyl D-aspartate 1a; grin2b: glutamate receptor, ionotropic, N-methyl D-aspartate 2b; trpv1: transient receptor potential cation channel, subfamily V, member 1; trpv4: transient receptor potential cation channel, subfamily V, member 4.

	β-act	gria1a	gria2a	gria3b	grin1a	grin2b	trpv1	trpv4
Slope	−3.39456	−3.56362	−3.46967	−3.49979	−3.386	−3.62188	−3.5275	−3.4511
Efficiency	1.970558	1.908153	1.941832	1.930775	1.97	1.888424	1.920821	1.948779
Efficiency (%)	98.53	95.41	97.09	96.54	98.50	94.42	96.04	97.44
Intercept	25.0553	32.42231	31.43253	31.88457	31.49	33.57191	33.65157	34.94192
Correl. coeff.	0.999141	0.999793	0.998933	0.998795	0.997	0.994216	0.985861	0.994338

was more prominent at 3 dpf, a developmental stage where the larvae are freely swimming and can be observed to exhibit epileptiform activity upon exposure to a convulsant agent (Baraban et al., 2007). Starting at 4 dpf, all *gria* and *grin* sub-types exhibit a significant increase in expression that steadily increases through 7 dpf. After 7 dpf the food sac is depleted and larvae require an exogenous source

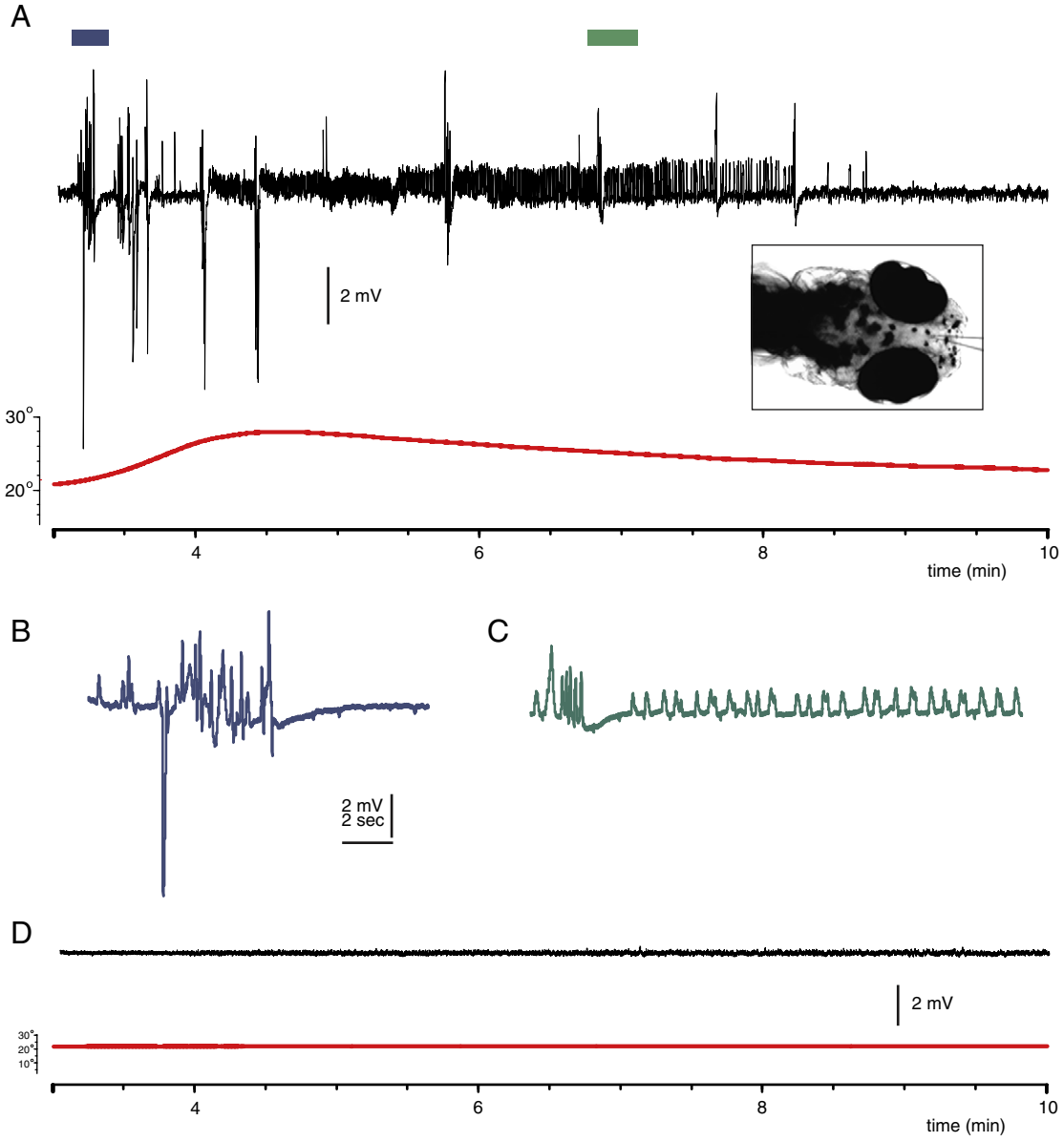

Fig. 1. Electrographic seizures in zebrafish larvae exposed to hyperthermia. (A) Representative extracellular field recording during transient elevation of bath temperature. Top trace shows the emergence of large ictal-like multi-spike burst discharge activity followed by mix of ictal-like and rapid short-duration interictal-like activity that returns to baseline levels when bath temperature decreases to room temperature. Bottom trace shows the change in bath temperature measured using a probe placed in the agar near the embedded zebrafish. Temperature was controlled by an in-line heater and external voltage source that was activated for 3 min. A representative recording configuration is shown in the frame-grabber image (*inset*). (B) High resolution trace showing ictal-like burst discharge; indicated as blue box in A. (C) High resolution trace showing interictal-like bursting; indicated as green box in A. (D) Representative field recording activity at room temperature; tectal recording (*top trace*), and bath temperature (*bottom trace*).

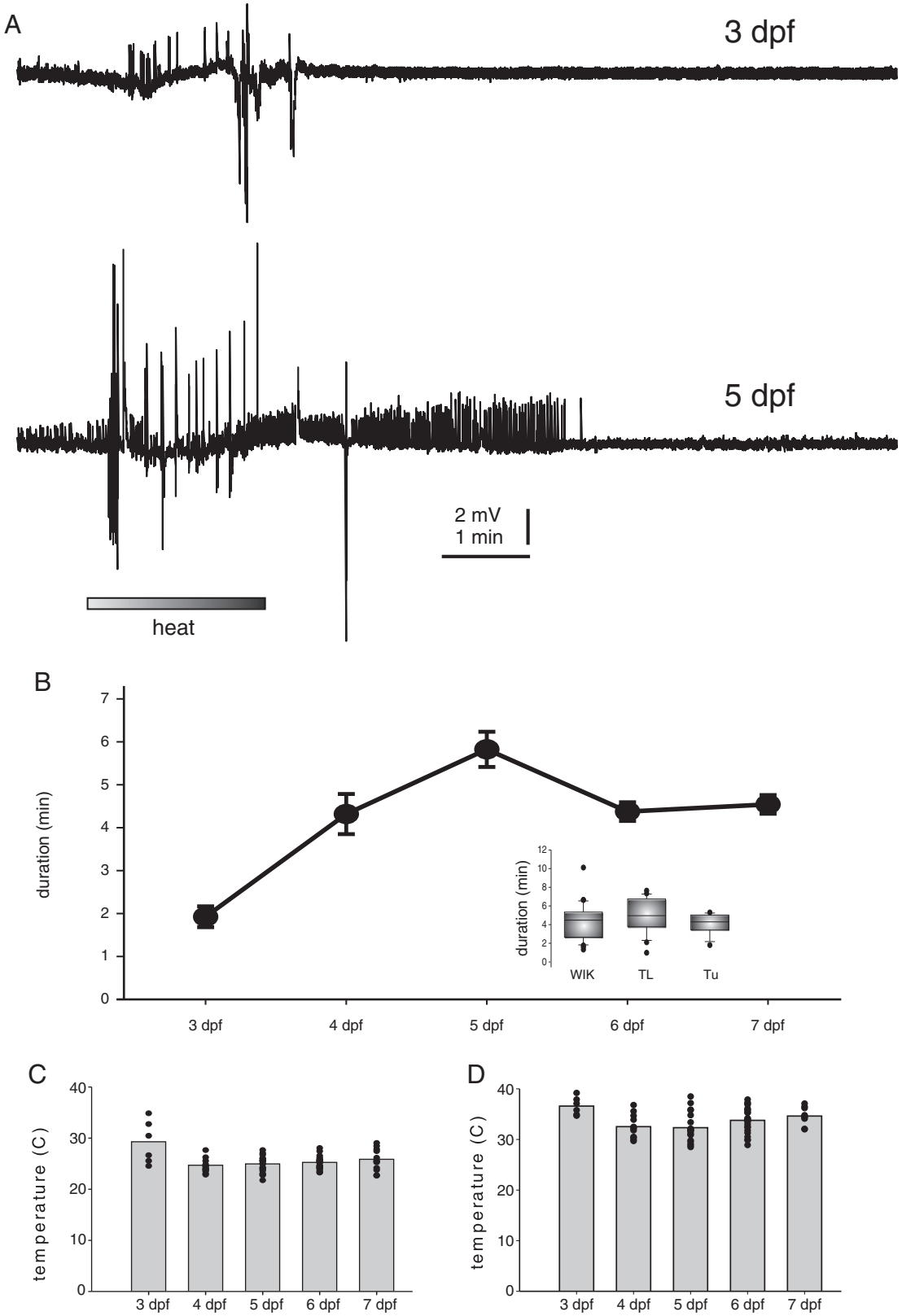

Fig. 2. Age dependence of hyperthermia-induced seizures in larval zebrafish. (A) Representative HT seizures elicited in larval zebrafish at 3 (top trace) and 5 dpf (bottom trace). (B) Plot of seizure duration versus developmental stage. Circles represent mean ± S.E.M. at each dpf. Box plot (inset) shows seizure durations for different wild-type strains during HT-induced seizures. (C) Plot of threshold temperature at which the first sign of an electrographic seizure was noted. Bars represent the mean temperature for each dpf; circles show individual experiments for each dpf. (D) Plot of the peak temperature reached during a hyperthermic challenge; same as in C.

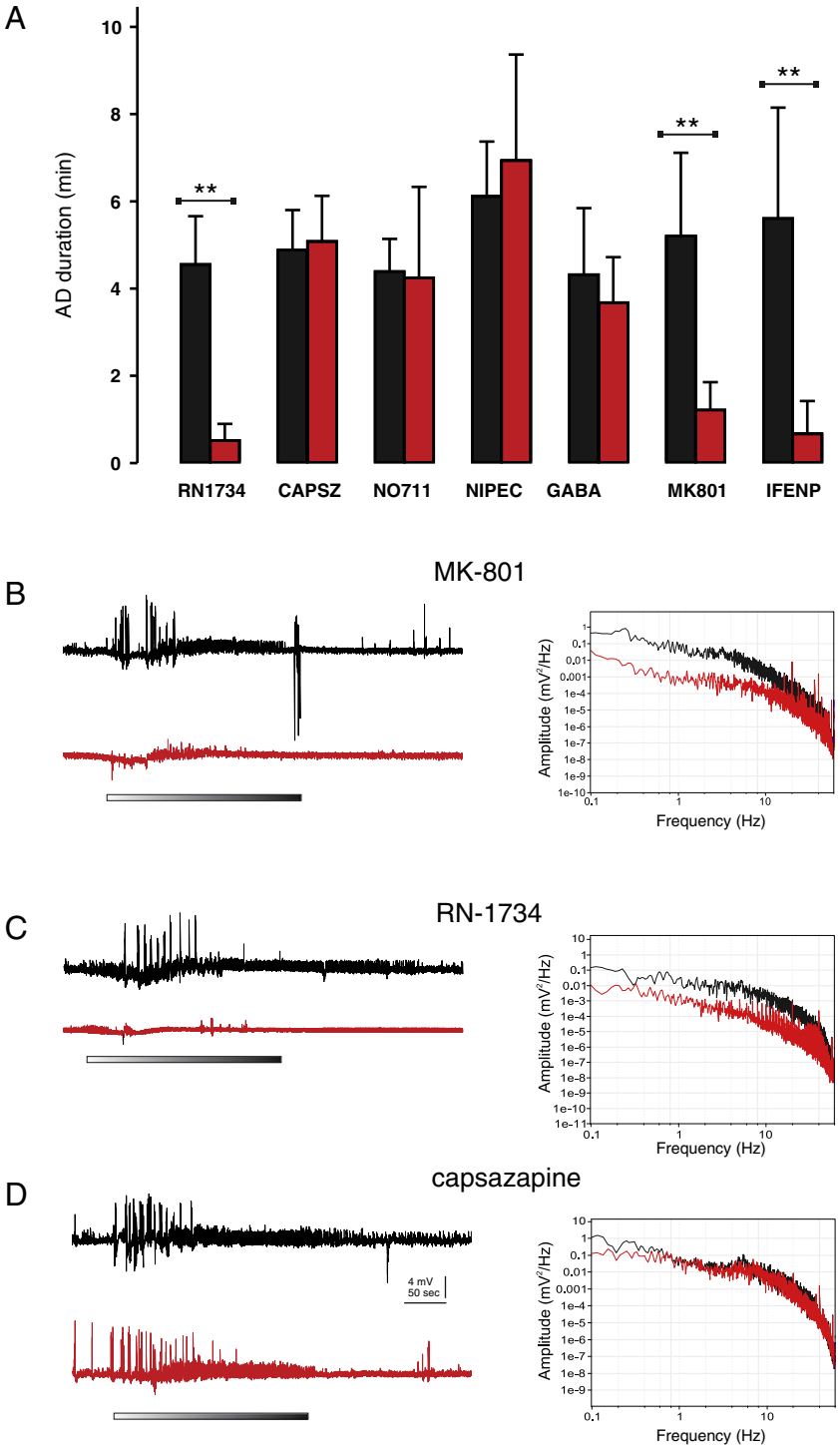

Fig. 3. Pharmacology of hyperthermia-induced seizures in larval zebrafish. (A) Bar plots of HT-induced seizure after discharge (AD) at baseline (black) and following application of a drug (red). Bars represent mean values ± S.D. N values represent the number of fish. RN1734 (N = 4; p = 0.029); CAPSZ, capsazapine (N = 3; p = 0.815), NO-711 (N = 4; p = 0.343), NIPEC, nipecotic acid (N = 5; p = 0.520), GABA (N = 5; p = 0.458), MK-801 (N = 6; p = 0.0006); IFENP, infenprodil (N = 5; p = 0.008). **significance $p \leq 0.05$. (B) Sample recordings are shown for a typical MK-801 experiment. Top trace represents the baseline HT; bottom trace is the same fish ~45 min after drug administration. Heat challenge shown as a bar below traces. Power spectrum for this experiment is shown in the plot at the right. (C) Same for RN-1374. (D) Same for capsazapine.

of nutrients; these ages are not reliable for electrophysiological studies and were not included in these studies. *trpv*1 and *trpv*4 channel expressions are also low at 2 and 3 dpf and increase with developmental stage between 4 and 7 dpf (Fig. 4C). qPCR data confirm the expression of these receptors and subunits at developmental stages where HT-induced seizures were elicited (see Fig. 2B) and pharmacological studies were performed (see Fig. 3A).

Discussion

Chronic changes in neuronal circuit function after experimental HT seizures have been described, but mechanisms underlying acute seizure generation during hyperthermia are not well understood. Here we show that a transient temperature increase evoked electrographic seizures in the CNS of developing zebrafish. This model of HT-induced

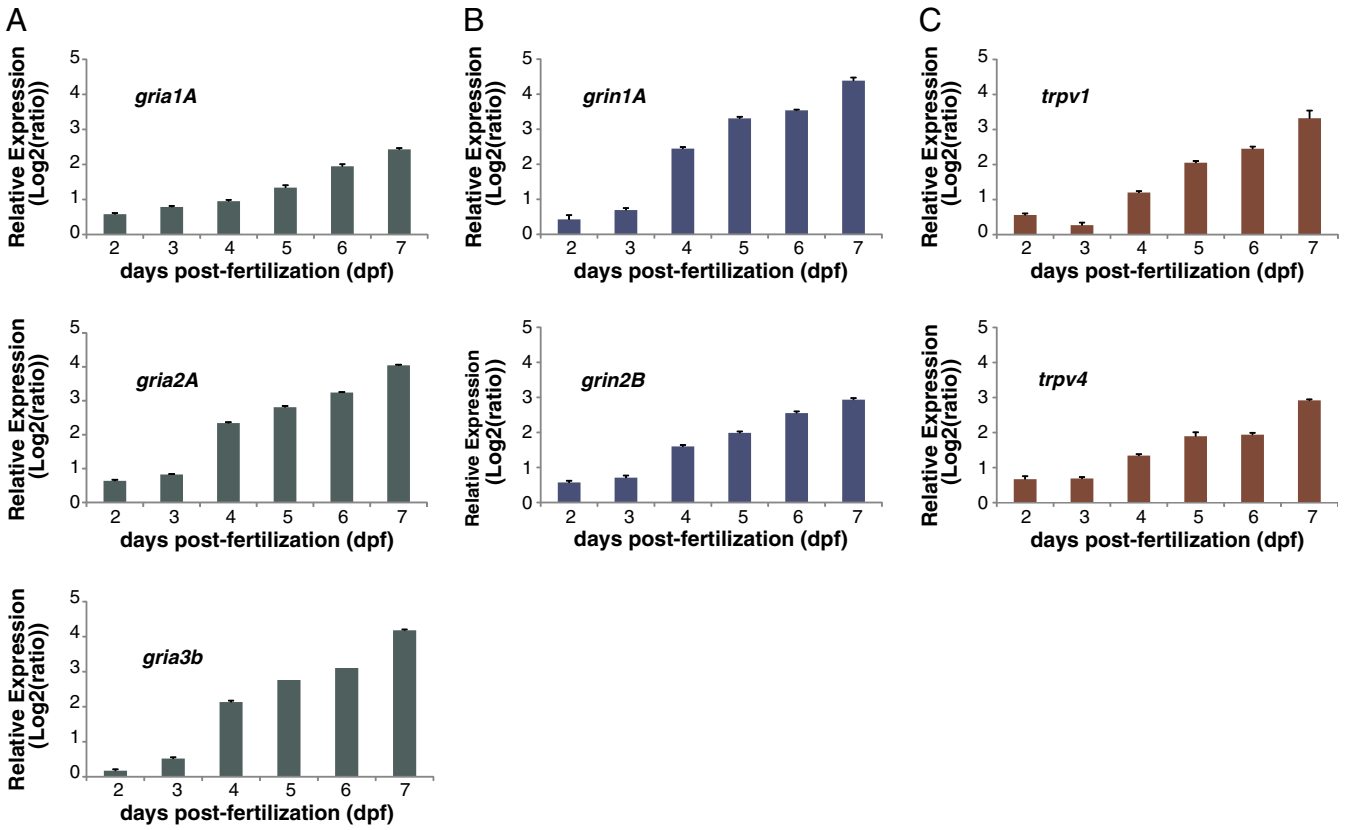

Fig. 4. Expression of TRPV channels and glutamate receptors in larval zebrafish. (A) Levels of mRNA (shown as mean ± S.E.M.), measured by qPCR were normalized to β-act and are shown for 2 through 7 dpf. (A) AMPA-type glutamate receptor subunits. (B) NMDA-type glutamate receptor subunits. (C) TRPV channels. gria1a: glutamate receptor, ionotropic, AMPA 1a; gria2a: glutamate receptor, ionotropic, AMPA 2a; gria3b: glutamate receptor, ionotrophic, AMPA; grin1a: glutamate receptor, ionotropic, N-methyl D-aspartate 1a; grin2b: glutamate receptor, ionotropic, N-methyl D-aspartate 2b; trpv1: transient receptor potential cation channel, subfamily V, member 1; and trpv4: transient receptor potential cation channel, subfamily V, member 4.

seizures recapitulates key features of febrile seizures in humans and rodents including age-dependence (Baram et al., 1997), a lack of strain differences (Dubé et al., 2004), reproducibility (Dubé and Baram, 2006), and the absence of mortality (Baram et al., 1997). Using a zebrafish model of hyperthermic seizures may provide experimental advantages over rodent models for examining acute mechanisms of seizure generation in vivo. Hyperthermia induction can be easily managed by controlling bath temperature via artificial heat ramp, drugs added to the bathing medium are easily absorbed, and electrographic seizure monitoring can be performed simultaneously on intact fish. Moreover, the rapid and external development, transparency, large clutch sizes, and the relatively large number of genetic tools available in zebrafish allow for detailed examination of structure–function relationships in vivo during or following hyperthermia exposure. These features might be especially beneficial for investigating the potential genetic or developmental basis of hyperthermic seizures, which are increasingly recognized as risk factors for febrile seizures (Hirose et al., 2003; Kira et al., 2010).

Our findings reveal a novel mechanism of HT-induced seizures via TRPV4 channels. It is well known that TRPV channels are sensitive to changes in temperature (Kauer and Gibson, 2009; Patapoutian et al., 2003), and their role in hyperthermic seizures has been speculated, but not experimentally tested (Dubé et al., 2009a). TRPV are non-selective cation channels with high Ca^{2+} permeability (Kauer and Gibson, 2009; Patapoutian et al., 2003), and their activation typically promotes glutamate release by increasing the excitability of neurons and synaptic terminals. Seizure onset in zebrafish was around 26 °C, which is near the reported temperature threshold for TRPV4 channel activation (24–34 °C) (Güler et al., 2002; Kauer and Gibson, 2009; Patapoutian et al., 2003; Shibasaki et al., 2007), and HT-induced seizures were almost completely blocked by a TRPV4 channel antagonist, RN-1734. Moreover, we showed that the age-dependence of HT seizure susceptibility mimicked the mRNA expression of TRPV4 and glutamate receptors. In zebrafish larvae, *trpv4* mRNA expression, assessed using in situ hybridization techniques, is prominent in the brain and head structures as early as 3 dpf (Mangos et al., 2007). Although TRPV4 is normally active at physiological temperatures, heat-evoked current amplitude through TRPV4 channels continues to increase as temperature rises, with a maximal activation around 42 °C (Güler et al., 2002; Shibasaki et al., 2007); and TRPV4-mediated current can fluctuate with suprathreshold temperature fluctuations between 36 and 42 °C (i.e., between normal temperature and fever) (Güler et al., 2002). Perhaps these features might partially explain the increased risk for febrile seizure with higher peak temperatures during fever. It is unlikely that TRPV channels were nonspecifically activated by hyperthermia. Seizure onset occurred far below the reported activation temperature for TRPV1 (>42 °C), TRPV2 (>52 °C), and TRPV3 (>35 °C) (Caterina et al., 1997; Kauer and Gibson, 2009; Patapoutian et al., 2003), and the TRPV1 channel specific antagonist, capsazapine, did not have an effect on HT seizures. It is also unlikely that febrile seizures in humans are mediated by TRPV1, because TRPV1 channels are not heavily expressed in human brain (Cavanaugh et al., 2011). Therefore, identification of TRPV4 channels represents a novel target for febrile seizures that might be useful for preventing seizures at the time of fever or reducing the duration/severity of prolonged seizures, which are known to promote subsequent epileptogenesis (Annegers et al., 1987; Dubé et al., 2006) or cognitive disabilities (Dubé et al., 2009b).

HT-induced seizure durations were also attenuated by the addition of post-synaptic glutamate receptor antagonists MK-801 and ifenprodil. Previous hypotheses about febrile seizure generation

have included enhanced NMDA receptor-mediated glutamate transmission (Morimoto et al., 1993, 1995) and changes in calcium homeostasis (Laorden et al., 1990). However, whether these mechanisms are directly involved in HT seizure generation has been considered controversial (Baram, 2002), because the pharmacological agents used to prevent HT-induced seizures in these studies also increased the threshold temperature for seizure onset. We found that reduced HT seizure durations were not accompanied by a change in the temperature of seizure onset in our zebrafish model. This finding supports a role of glutamatergic transmission by NMDA type glutamate receptors in HT seizure generation or spread. Interestingly, a previous study showed that temperature-activation of TRPV4 channels depolarized the resting membrane potential of cultured hippocampal pyramidal neurons and partially relieved the Mg^{2+} block of NMDA receptors (Shibasaki et al., 2007). However, it remains unknown if the response of TRPV4 channels to hyperthermia directly involves NMDA receptor activation, acts in a convergent manner, or reflects separate mechanisms. Nonetheless, acute HT-induced seizures appear to involve increased activities of both TRPV4 channels and post-synaptic NMDA-type glutamate receptors.

References

Annegers, J.F., Hauser, A., Shirts, S.B., Kurland, L.T., 1987. Factors prognostic of unprovoked seizures after febrile convulsions. N. Engl. J. Med. 316, 493–498.

Baraban, S.C., Taylor, M.R., Baier, H., 2005. Pentylenetetrazole induced changes in zebrafish behavior, neural activity and c-fos expression. Neuroscience 131, 759–768.

Baraban, S.C., Dinday, M.T., Castro, P.A., Chege, S., Guyenet, S., Taylor, M.R., 2007. A large-scale mutagenesis screen to identify seizure-resistant zebrafish. Epilepsia 48, 1151–1157.

Baram, T.Z., 2002. Animal models of febrile seizures. In: Baram, T.Z., Shinnar, S. (Eds.), Febrile Seizures. Academic Press, pp. 189–202.

Baram, T.Z., Angelika, G., Schultz, L., 1997. Febrile seizures: an appropriate-aged model suitable for long-term studies. Brain Res. Dev. Brain Res. 96, 265–270.

Benfenati, V., Amiry-Moghaddam, M., Caprini, M., Mylonakou, M.N., Rapisarda, C., Op, Ottersen, Ferroni, S., 2007. Expression and functional characterization of transient receptor potential vanilloid-related channel 4 (TRPV4) in rat cortical astrocytes. Neuroscience 4, 876–892.

Berg, A.T., Shinnar, S., Hauser, W.A., Alemany, M., Shapiro, E.D., Salomon, M.E., Crain, E.F., 1992. A prospective study of recurrent febrile seizures. N. Engl. J. Med. 327, 1122–1127.

Berg, A.T., Shinnar, S., Darefsky, A.S., Holford, T.R., Shapiro, E.D., Salomon, M.E., Crain, E.F., Hauser, A.W., 1997. Predictors of recurrent febrile seizures. A Prospective cohort study. Arch. Pediatr. Adolesc. Med. 151, 371–378.

Bhaskaran, M.D., Smith, B.N., 2010. Effects of TRPV1 activation on synaptic excitation in the dentate gyrus of a mouse model of temporal lobe epilepsy. Exp. Neurol. 223, 529–536.

Brewster, A., Bender, R.A., Chen, Y., Dube, C., Eghbal-Ahmadi, M., Baram, T.Z., 2002. Developmental febrile seizures modulate hippocampal gene expression of hyperpolarization-activated channels in an isoform- and cell-specific manner. J. Neurosci. 22, 4591–4599.

Caterina, M.J., Schumacher, M.A., Tominaga, M., Rosen, T.A., Levine, J.D., Julius, D., 1997. The capsaicin receptor: a heat-activated ion channel in the pain pathway. Nature 389, 816–824.

Cavanaugh, D.J., Chesler, A.T., Jackson, A.C., Sigal, Y.M., Yamanaka, H., Grant, R., O'Donnell, D., Nicoll, R.A., Shah, N.M., Julius, D., Basbaum, A.I., 2011. Trpv1 reporter mice reveal highly restricted brain distribution and functional expression in arteriolar smooth muscle cells. J. Neurosci. 31, 5067–5077.

Chege, S.W., Hortopan, G.A., Dinday, M.T., Baraban, S.C., 2012. Expression and function of KCNQ channels in larval zebrafish. Dev. Neurobiol. 72, 186–198.

Chen, K., Baram, T.Z., Soltesz, I., 1999. Febrile seizures in the developing brain result in persistent modification of neuronal excitability in limbic circuits. Nat. Med. 5, 888–894.

Chen, K., Aradi, I., Thon, N., Eghbal-Ahmadi, M., Baram, T.Z., Soltesz, I., 2001. Persistently modified h-channels after complex febrile seizures convert the seizure-induced enhancement of inhibition to hyperexcitability. Nat. Med. 7, 331–337.

Doyle, M.W., Bailey, T.W., Jin, Y.H., Andresen, M.C., 2002. Vanilloid receptors presynaptically modulate cranial visceral afferent synaptic transmission in nucleus tractus solitarius. J. Neurosci. 22, 8222–8229.

Dubé, C.M., Baram, T.Z., 2006. Complex febrile seizures - an experimental model in immature rodent. In: Pitkanen, A., Schwartzkroin, P.A., Moshe, S.L. (Eds.), Models of Seizures and Epilepsy. Elsevier, San Diego, pp. 333–340.

Dubé, C., Vezzani, A., Behrens, M., Bartfai, T., Baram, T.Z., 2004. Interleukin-1β contributes to the generation of experimental febrile seizures. Ann. Neurol. 57, 152–155.

Dubé, C., Richichi, C., Bender, R.A., Chung, G., Litt, B., Baram, T.Z., 2006. Temporal lobe epilepsy after experimental prolonged febrile seizures: prospective analysis. Brain 129, 911–922.

Dubé, C.M., Brewster, A.L., Richichi, C., Zha, Q., Baram, T.Z., 2009a. Fever, febrile seizures and epilepsy. Trends Neurosci. 30, 490–496.

Dubé, C.M., Zhou, J.L., Hamamura, M., Zhao, Q., Ring, A., Abrahams, J., McIntyre, K., Nalcioglu, O., Shatskih, T., Baram, T.Z., Holmes, G.L., 2009b. Cognitive dysfunction after experimental febrile seizures. Exp. Neurol. 215, 167–177.

Dubé, C.M., Ravizza, T., Hamamura, M., Zha, Q., Keebaugh, A., Fok, K., Andres, A.L., Nalcioglu, O., Obenaus, A., Vezzani, A., Baram, T.Z., 2010. Epileptogenesis provoked by prolonged experimental febrile seizures: mechanisms and biomarkers. J. Neurosci. 30, 7484–7494.

Güler, A.D., Lee, H., Iida, T., Shimizu, I., Tominaga, M., Caterina, M., 2002. Heat-evoked activation of the ion channel, TRPV4. J. Neurosci. 22, 6408–6414.

Hauser, W., Hersdorffer, D., 1990. Epilepsy: frequency, causes and consequences. Demos, New York.

Hirose, S., Mohney, R.P., Okada, M., Kaneko, S., Mitsudome, A., 2003. The genetics of febrile seizures and related epilepsy syndromes. Brain Dev. 25, 304–312.

Jin, Y.H., Bailey, T.W., Li, B., Schild, J.H., Andresen, M.C., 2004. Purinergic and vanilloid receptor activation releases glutamate from separate cranial afferent terminals in nucleus tractus solitarius. J. Neurosci. 24, 4700–4717.

Kauer, J.A., Gibson, H.E., 2009. Hot flash: TRPV channels in the brain. Trends Neurosci. 32, 215–224.

Kira, R., Ishizaki, Y., Torisu, H., Sanefuji, M., Takemoto, M., Sakamoto, K., Matsumoto, S., Yamaguchi, Y., Yukaya, N., Sakai, Y., Gondo, K., Hara, T., 2010. Genetic susceptibility to febrile seizures: case–control association studies. Brain Dev. 32, 57–63.

Laorden, M.L., Carrillo, E., Miralles, F.S., Puig, M.M., 1990. Effects of diltiazem on hyperthermia induced seizures in the rat pup. Gen. Pharmacol. 21, 313–315.

Livak, K.J., Schmittgen, T.D., 2001. Analysis of relative gene expression data using real-time quantitative PCR and the 2(-Delta Delta C (T)) method. Methods 25, 402–408.

Mangos, S., Liu, Y., Brummond, I.A., 2007. Dynamic expression of the osmosensory channel trpv4 in multiple developing organs in zebrafish. Mol. Biol. Cell 7, 480–484.

Morimoto, T., Nagao, H., Yoshimatsu, M., Yoshida, K., Matsuda, H., 1993. Pathogenic role of glutamate in hyperthermia induced seizures. Epilepsia 34, 447–452.

Morimoto, T., Kida, K., Nagao, H., Yoshida, K., Fukuda, M., Takashima, S., 1995. The pathogenic role of the NMDA receptor in hyperthermia-induced seizures in developing rats. Brain Res. Dev. Brain Res. 84, 204–207.

Patapoutian, A., Peier, A.M., Story, G.M., Viswanath, V., 2003. Thermotrep channels and beyond: mechanisms of temperature sensation. Nat. Rev. Neurosci. 4, 529–539.

Peters, J.H., McDougall, S.J., Fawley, J.A., Smith, S.M., Andresen, M.C., 2010. Primary afferent activation of thermosensitive TRPV1 triggers asynchronous glutamate release at central synapses. Neuron 65, 657–669.

Pfaffi, M.W., 2001. A new mathematical model for relative quantification in real-time RT-PCR. Nucleic Acids Res. 29, e45.

Richichi, C., Brewster, A.L., Bender, R.A., Simeone, T.A., Zha, Q., Yin, H.Z., Weiss, J.H., Baram, T.Z., 2008. Mechanisms of seizure-induced 'transcriptional channelopathy' of hyperpolarization-activated cyclic nucleotide gated (HCN) channels. Neurobiol. Dis. 29, 297–305.

Saito, S., Shingai, R., 2006. Evolution of thermoTRP ion channel homologs in vertebrates. Physiol. Genomics 27, 219–230.

Shibasaki, K., Suzuki, M., Mizuno, A., Tominaga, M., 2007. Effects of body temperature on neural activity in the hippocampus: regulation of resting membrane potentials by transient receptor potential vanilloid 4. J. Neurosci. 27, 1566–1575.

Shinnar, S., 1998. Prolonged febrile seizures and mesial temporal sclerosis. Ann. Neurol. 43, 411–412.

Stafstrom, C.E., 2002. The incidence and prevalence of febrile seizures. In: Baram, T.Z., Shinnar, S. (Eds.), Febrile Seizures. Academic Press, pp. 1–25.

Tancredi, V., D'Arcangelo, G., Zona, C., Siniscalchi, A., Avoli, M., 1992. Induction of epileptiform activity by temperature elevation in hippocampal slices from young rats: an in vitro model for febrile seizures? Epilepsia 33, 228–234.

Tsai, M.L., Leung, L.S., 2006. Decrease of hippocampal $GABA_B$ receptor-mediated inhibition after hyperthermia-induced seizures in immature rats. Epilepsia 47, 277–287.

Verity, C.M., Butler, N.R., Golding, J., 1985. Febrile convulsions in a national cohort followed up from birth. Prevalence and recurrence in the first five years of life. Br. Med. J. 290, 1307–1310.

Westerfield, M., 1993. The zebrafish book : a guide for the laboratory use of zebrafish (Brachydanio rerio). M. Westerfield, Eugene, OR.

Wu, J., Fisher, R.S., 2000. Hyperthermic spreading depression in the immature rat hippocampal slice. J. Neurophysiol. 84, 1355–1360.

Zsombok, A., Bhaskaran, M.S., Gao, H., Derbenev, A.V., Smith, B.N., 2012. Functional plasticity of central TRPV1 receptors in brainstem dorsal vagal complex circuits of streptozotocin-treated hyperglycemic mice. J. Neurosci. 31, 14024–14031.